Supplemental Materials

A common single nucleotide variant in the cytokine receptor-like factor-3 (CRLF3) gene causes neuronal deficits in human and mouse cells

Anna F. Wilson, Rasha Barakat, Rui Mu, Leah L. Karush, Yunqing Gao, Kelly A. Hartigan, Ji-Kang Chen, Hongjin Shu, Tychele N. Turner, Susan E. Maloney, Steven J. Mennerick, David H. Gutmann, Corina Anastasaki

Supplemental Methods

Maternal Isolation-induced Ultrasonic Vocalizations. During the first two postnatal weeks, we assessed *Crlf3*$^{+/m}$ and wild type (WT) littermates in cohort 1 for signs of gross developmental delay, communicative delay or motor delay, using previously published methods (1). To evaluate gross development, mice were weighed on each day of testing from postnatal day (PND; P) P6 - P14, and evaluated for physical milestones of development, including pinna detachment by P6 and eye opening by P14. Ultrasonic vocalizations (USVs) produced by mouse pups during the first two weeks of life are one of the earliest forms of social communication in mice, and these isolation calls elicit maternal care from the dam (2). Tissue was collected from all pups on P5 for genotyping. USVs were recorded on P6, P8, and P10 following previously published methods (1, 3). Briefly, the dam was removed from the nest and the litter placed on a warming pad to maintain body temperature. The surface temperature of each pup was recorded (HDE Infrared Thermometer; WT: M=35°C, SD=1.05; Crlf3+/m: M=35.3°C, SD=1.22) prior to placement in an empty polycarbonate cage (28.5 x 17.5 x 12 cm) within a sound-attenuating chamber. USVs were recorded for three minutes using an Avisoft UltraSoundGate CM16 microphone, Avisoft UltraSoundGate 116H amplifier, and Avisoft Recorder software (gain = 8 dB, 16 bits, sampling rate = 250 kHz). The pup was then weighed and returned to the nest. The dam was returned to the nest following recording of the last pup in the litter. Frequency sonograms were prepared from recordings using MATLAB (frequency range = 25 kHz to 120 kHz, FFT size = 512, overlap = 50%, time resolution = 1.024 ms, frequency resolution = 488.2 Hz). Individual syllables and other spectral features were identified and counted from the sonograms, as previously described (4, 5). To assess achievement of motor milestones, the surface righting reflex was assessed for each pup at P14 (1). Each pup was placed on its back in an empty cage lined with a plastic bench pad and the time to return to a prone position was recorded for up to 60 sec. Three trials were conducted and averaged for analysis.

Social Approach. The three chamber social approach (6) task was used to assess sociability and preference for social novelty at P29 in cohort 2 using procedures previously described (1). Sociability is defined as the preference to spend time with a novel conspecific over a novel empty cup. Social novelty is defined as the preference to spend time with a novel versus familiar conspecific object. Stimulus partner mice were sex-, age- and strain-matched. The full acrylic apparatus measured 60cm x 40cm x 20cm divided equally into three chambers separated by acrylic walls. Two stainless steel cages (Galaxy Pencil/Utility Cup, Spectrum Diversified Designs, Inc.), measuring 10 cm tall and 10 cm in diameter with vertical bars, served as conspecific stimulus cages and allowed for controlled, minimal contact interactions between experimental and stimulus mice. Behavior of the animals was tracked using Any-maze tracking software (Stoelting, Co; http://www.anymaze.co.uk) to quantify distance traveled, time spent in and entries into each chamber and investigation zone. An investigation zone was defined as the area 2 cm outward from the perimeter of each conspecific cage. An entry into the investigation zone requires the nose-point to be within the zone, constituting a purposeful interaction by the test mouse. The social preference score was calculated as (time in social / (time in social + time in empty))*100. The novelty preference score was calculated as (time in novel / (time in novel + time in familiar))*100. Statistical analysis was as previously described (7). Testing consists of four, consecutive 10-minute trials. Trials 1 and 2 habituate the test mouse to the center chamber and the whole apparatus with stimulus cups, respectively. Trials 3 and 4 test sociability (novel mouse vs. empty cup) and social novelty preference (novel mouse vs. familiar mouse), respectively. Between animals, the stimulus cups were cleaned with 70% ethanol and the acrylic apparatus was cleaned with 0.02% chlorhexidine diacetate solution.

Elevated Plus Maze. Anxiety-like avoidance behaviors were tested at P40 and P35 in cohorts 2 and 3, respectively, using the Elevated Plus Maze (EPM) as previously described (8, 9). Briefly, mice were placed in the center of the apparatus, which contained two open and two closed arms, and allowed to explore for 5 minutes in the dark. This was repeated for two more days. Outcomes were averaged across days for analysis. MotorMonitor software (Kinder Scientific, LLC, Poway, CA) quantified beam breaks as duration, distance traveled, entries, and time at rest in each zone (closed arms, open arms and center area).

1-hr Locomotor Activity & Exploration. General locomotor activity and exploration were evaluated at P45 in cohort 2 for 1 hour in polycarbonate enclosures (47.6 × 25.4 × 20.6 cm) surrounded by metal frames containing 4 × 8 matrices of photo beam pairs as previously described (9). MotorMonitor Software (Kinder Scientific, LLC, Poway, CA) quantified horizontal and vertical beam breaks as ambulations and rearing, respectively. General activity variables (total ambulations, rearing, time at rest) along with time spent, distance traveled and entries made into the 33cm × 11cm central zone were analyzed.

Rotarod. Motor coordination was assessed at P50 in cohort 2 using the Rotarod (Rotamex-5; Columbus Instruments, Columbus, OH), as previously reported (9). Briefly, latency to fall was measured for each mouse in three different situations: a stationary rod (for up to 60 sec), a continuously rotating rod (2.5 rpm; for up to 60 sec), and an accelerating rod (0.13 rpm acceleration for 180 seconds). Each mouse received one stationary, two continuous, and two accelerating trials on each of three test days. Tests were separated by three days.

Self-grooming. Spontaneous self-grooming in a novel environment was assessed at P70 in cohort 2. Each mouse was placed in a clean, empty polycarbonate cage (28.5 x 17.5 x 12 cm) inside a clear acrylic enclosure measuring 28 cm x 17.5 cm x 37.5 cm with a 4-cm diameter top hole allowing for placement of a digital video camera (Sony HDR-Cx560V High Definition Handycam camcorder). The behavior of the animal was video recorded for ten minutes. Video recordings were post-processed using Movavi video

editor (http://www.movavi.com) to adjust for brightness and contrast to enable optimal behavior tracking with Ethovision XT (Noldus). Grooming frequency and duration were quantified using the Behavior Recognition Module (BMR; Ethovision, XT, Noldus). To determine probability and threshold parameters for BRM, a subset of videos was manually scored by an independent experimenter highly trained in assessments of grooming, and intraclass correlation coefficients (ICC) were used to determine inter-rater reliability of grooming measurements produced by the independent experimenter and Ethovision XT scoring. Excellent correlations (ICC = .995) were achieved for both duration and frequency for grooming probability at or above 40% with a behavior threshold of 2 seconds. These parameters were used to extract the data from Ethovision.

Light/ Dark Box. The Light/Dark Box was used to assess anxiety-related avoidance behavior leveraging the mouse's innate preference for dark spaces at P32 in cohort 3. Mice were placed in the dark side of a chamber (47.6 x 25.4 x 20.6 cm) and were allowed to explore freely. The light side, which was twice the size of the dark side, was illuminated at 65 lux with incandescent desk lamps. Beam brakes were used to measure time spent in each chamber during the 6-minute task. For the first two minutes, mice were confined to the dark side of the apparatus, and then allowed to explore the entire apparatus for the remaining four minutes. Time spent in and latency to move to the light side during the latter four minutes were used as a proxy for anxiety-like behavior.

Open Field. At P39 in cohort 3, ambulatory activity, exploratory, and avoidance-related behaviors were assessed in an open field (41 x 41 x 38.5 cm high) apparatus constructed of acrylic and surrounded by metal frames containing 16 x 16 matrices of photocell pairs as previously described (10). MotorMonitor Software (Kinder Scientific, LLC, Poway, CA) quantified general activity variables included total ambulations (whole body movements), vertical rearing frequency, and distance traveled in a 5.1 cm wide peripheral zone that surrounded the field. Classic measures of open area avoidance behavior included quantifying

time spent in, distance travelled in, and number of entries made into a 10.2 x 10.2 cm central zone of the field.

Fear Conditioning. Associative anxiety-related memory was assessed at P49 in cohort 3 in the conditioned fear task. The procedure was conducted using the Actimetrics conditioning system (Wilmette, IL, USA) as previously published (1). Briefly, following pairing of a tone and context with a 1.0 mA foot shock on day 1, mice were tested for contextual fear memory on day 2 and cued fear memory in response to the tone only on day 3. Sensitivity to foot shocks was assessed following the last day of conditioned fear testing to confirm that the differences in freezing behavior were not confounded by differences in reactivity to the shock current (8). Mice were placed in the fear conditioning chambers and exposed to 3s foot shocks every 20-30s starting at 0.05 mA and increasing in intensity by 0.05 mA until a flinch was elicited. The current at which each behavior occurred was recorded.

Supplemental Table S1. Genes with altered expression in hippocampal neurons from *Crlf3*$^{+/m}$ mice.

Genes with greater than 3-fold altered expression in hippocampal neurons from *Crlf3*$^{+/m}$ relative to WT mice using Hurdle model analysis. Only one gene had reduced expression (*Ttr*).

Feature ID	Ensembl ID	P-value (*Crlf3*$^{+/m}$ vs WT)	FDR step up (*Crlf3*$^{+/m}$ vs WT)	Ratio (*Crlf3*$^{+/m}$ vs WT)	Fold change (*Crlf3*$^{+/m}$ vs WT)
Fam172a	ENSMUSG00000064138	2.44E-05	1.54E-03	3.03E+00	3.03
Osbp	ENSMUSG00000024687	1.32E-06	1.20E-04	3.29E+00	3.29
Scand1	ENSMUSG00000046229	3.91E-06	3.20E-04	3.06E+00	3.06
Sf3a2	ENSMUSG00000020211	3.97E-08	4.38E-06	3.53E+00	3.53
Ttr	ENSMUSG00000061808	1.11E-16	1.73E-14	1.15E-01	-8.68

Supplemental Table S2. Upregulated pathways in hippocampal neurons from *Crlf3*$^{+/m}$ mice. Pathways and associated genes upregulated (FDR<0.1) in mouse *Crlf3*$^{+/m}$ hippocampal neurons relative to their WT counterparts using scSeq GO analysis.

Term	PValue	Genes	Fold Enrichment	Bonferroni	Benjamini	FDR
GO:0008380~RNA splicing	5.46E-05	XAB2, RBM15B, IK, PRPF39, SF3A2, FAM172A, SCAF11, CWC15, SCAF1, CRNKL1	5.823352857	0.051360623	0.052725117	0.0527251
GO:0005737~cytoplasm	2.82E-06	RAB7, NUCKS1, LSM12, PPP3CB, MAEA, RARS, RFK, OSBP, AKT3, FBXO3, TXNL4A, KPNA3, APPL1, ACTR3, MAGI1, IK, TPM3, NGDN, TSC2, LARP4B, FTSJ1, SREBF2, LATS1, SLC25A17, TRAF4, PSMA1, MAPKAPK2, WDFY3, CSNK1G2, VPS28, ARL8A, COX19, USP15, PSMD12, GDPD1, LIN7C, AK6, STIP1, COPI, PRDX5, EXOSC10, FAM172A, CSK, APBB1, MARK4, PAIP1, S100A10, ACBD6, SMAD4, DYNLT1B, AP5, YIPF3, BOD1, MCRS1, CRIPT, SOD2, CORO2B, HIPK2, SLC4A7, GLUD1, PAN3, STK25, FASN, PHF14, MDM2, EIF3G, SRPRB, PDCD2, SMAP1, MBTPS2	1.585850047	8.12E-04	5.62E-04	5.43E-04
GO:0005730~nucleolus	5.07E-06	SUZ12, MAGI1, SCAF11, MCRS1, NGDN, PPAN, NUCKS1, SSRP1, LARP4B, BAZ1B, PWP1, FBL, EXOSC10, SRP72, RARS, OSBP, MDM2, WDFY3, MAGED2	3.576930649	0.001458494	5.62E-04	5.43E-04
GO:0005634~nucleus	5.85E-06	ICE1, PPAN, NUCKS1, PWP1, PSMD8, FBL, MAEA, RARS, AKT3, FBXO3, TXNL4A, KPNA3, APPL1, ACTR3, MAGI1, SEC13, IK, EED, NGDN, UBE2QL1, TSC2, BAZ1B, CRNKL1, SREBF2, TRAF4, PSMA1, DMWD, MAPKAPK2, WDFY3, CSNK1G2, ZFP451, USP15, AK6, AGPAT3, PURB, STIP1, COPI, PRDX5, RBM15B, EXOSC10, FAM172A, NUP88, APBB1, SCAND1, SUZ12, SMAD4, PHC1, SF3A2, AP5, MCRS1, CWC15, FOXN3, SSRP1, SCAF1, HIPK2, XAB2, PRPF39, PHF14, MDM2, EIF3G, PDCD2, CEBPZ, MAGED2	1.637046781	0.001684668	5.62E-04	5.43E-04
GO:0001739~sex chromatin	5.09E-04	SUZ12, PHC1, EED	84.152	0.13638215	0.033432125	0.0322713
GO:0005681~spliceosomal complex	6.41E-04	XAB2, IK, SF3A2, AP5, CWC15, TXNL4A, CRNKL1	6.656090395	0.16859796	0.033432125	0.0322713
GO:0005654~nucleoplasm	6.97E-04	USP15, ICE1, NUCKS1, AK6, PURB, FBL, RBM15B, EXOSC10, MAEA, RARS, OSBP, FBXO3, NUP88, TXNL4A, KPNA3, SUZ12, MAGI1, IK, SMAD4, SEC13, PHC1, SCAF11, EED, MCRS1, NGDN, UBE2QL1, BAZ1B, SREBF2, HIPK2, XAB2, PSMA1, TRAF4, MAPKAPK2, MDM2, WDFY3, MAGED2	1.747100346	0.181811589	0.033432125	0.0322713
GO:0005694~chromosome	0.002032234	SUZ12, FBL, IK, BOD1, EED, NGDN, FBXO28, PHF14, NUCKS1, SSRP1, PWP1	3.247397193	0.443383533	0.083611903	0.0807087
GO:0000166~nucleotide binding	3.21E-04	ACTR3, MAGI1, RAB7, RAB5C, EFL1, UBE2QL1, BAZ1B, HIPK2, LATS1, GLUD1, EXOSC10, PAN3, STK25, RARS, RFK, MAPKAPK2, AKT3, SRPRB, CSK, EIF2S3Y, MARK4, CSNK1G2, ATP9A, ARL8A	2.230272654	0.09095213 2	0.09534222	0.0953422

Supplemental Table S3. Primary Antibodies Used

Antibody	Company	Catalog #	Dilution
Ankyrin-G	Thermo Scientific	33-8800	1:250
CRLF3	Sigma-Aldrich	HPA007596	1:100
GAPDH	Abcam	ab8245	1:10,000
Ki67	BD Biosciences	556003	1:100
MAP2 (ICC)	Abcam	ab5392	1:5000
MAP2 (IF; WB)	Abcam	ab11267	1:500
NeuN	Millipore	MAB377	1:500
NeuroD1	Abcam	ab205300	1:250
SMI-32	BioLegend	801701	2.5 µg/mL
SMI-312	BioLegend	837904	2.5 µg/mL
SOX2	Abcam	ab92494	1: 200
TBR1	Abcam	ab183032	1:50
TBR2	Abcam	ab261913	1:50
α-Tubulin	Abcam	ab176560	1:5,000
TUJ-1	Abcam	ab78078	1 µg/mL

Supplemental Table S4. Taqman Expression Assay Primers

Gene	**Taqman Accession Number**
Crlf3	Mm0065818_m1
CRLF3	Hs00367579_m1
Gapdh	Mm99999915_g1
GAPDH	Hs02786624_g1

Supplemental Figures

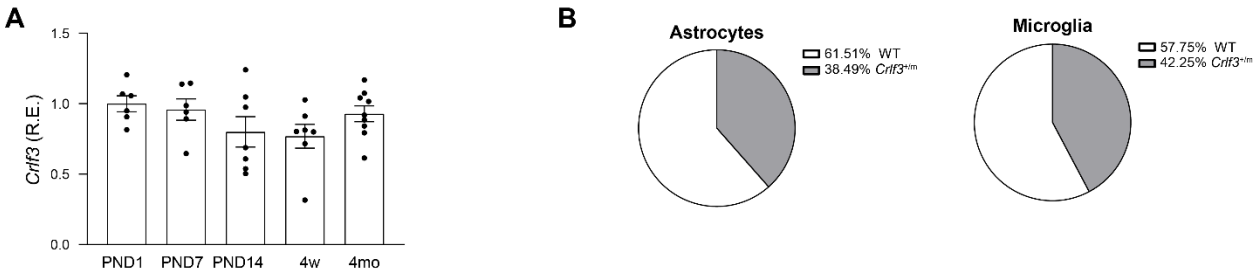

Supplemental Figure 1. Cellular and molecular analysis of WT and *Crlf3*$^{+/m}$ mouse brain

(**A**) Quantitative PCR of mouse hippocampi showing similar expression of *Crlf3* mRNA in WT mice at different ages. Each data point represents both hippocampi from one mouse. Data are shown as the mean ± SEM. (**B**) Following single cell RNAseq and exclusive analysis of hippocampal astrocytes (left) or microglia (right), WT and *Crlf3*$^{+/m}$ astrocytes and microglia are similarly represented by both genotypes.

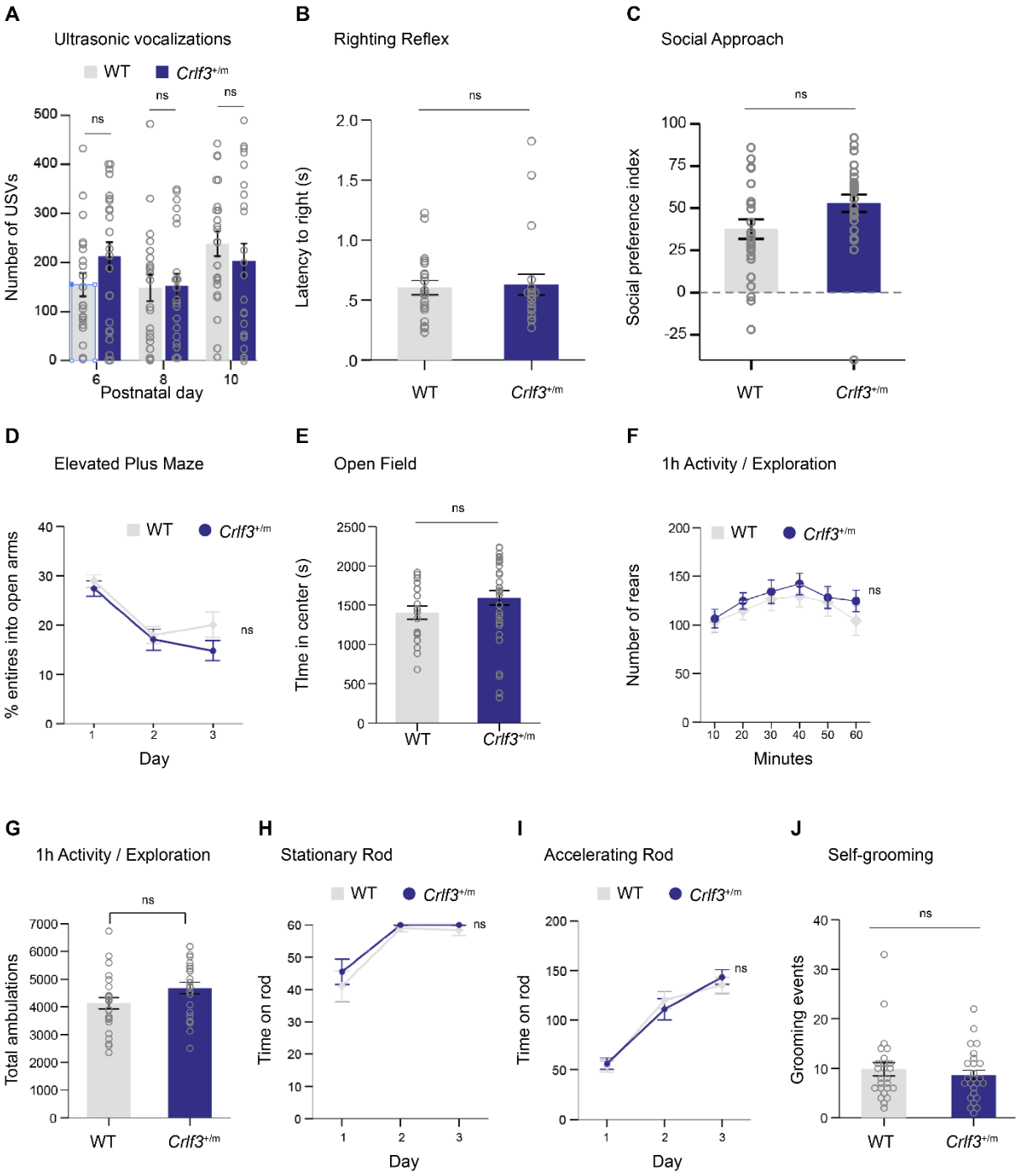

Supplemental Figure 2. Behavioral analyses of *Crlf3*$^{+/m}$ mice. Representative analyses from (**A**) ultrasonic vocalization recordings, (**B**) righting reflex recordings, (**C**) social approach analyses, (**D**) elevated-plus maze testing, (**E**) open field test analysis, (**F-G**) 1h activity/exploration testing, (**H-I**) stationary and accelerating Rotarod testing, and (**J**) self-grooming behavior recordings reveal no deficits in *Crlf3*$^{+/m}$ mice relative to their wild type littermates. ns, not significant.

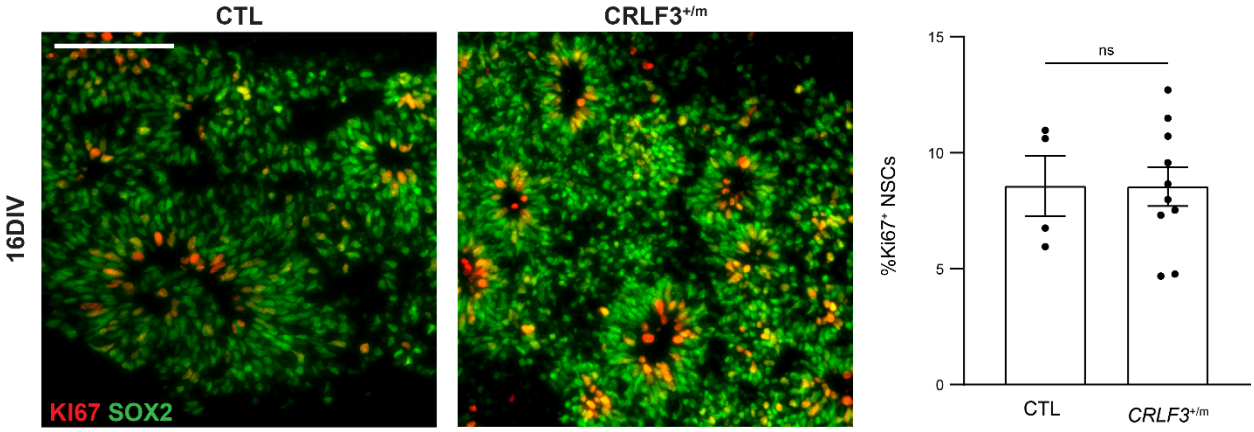

Supplemental Figure 3. *CRLF3*$^{+/m}$ hCOs proliferate at similar rates as control hCOs. Representative images of immunofluorescent staining and quantification of Ki67^{+} NSCs (SOX2^{+}), showing similar proliferation of CTL and *CRLF3*$^{+/m}$ hCOs at 16DIV. All data are shown as the mean ± SEM. Statistical analysis by unpaired, two-tailed t-test with Welch's correction. ns, not significant.

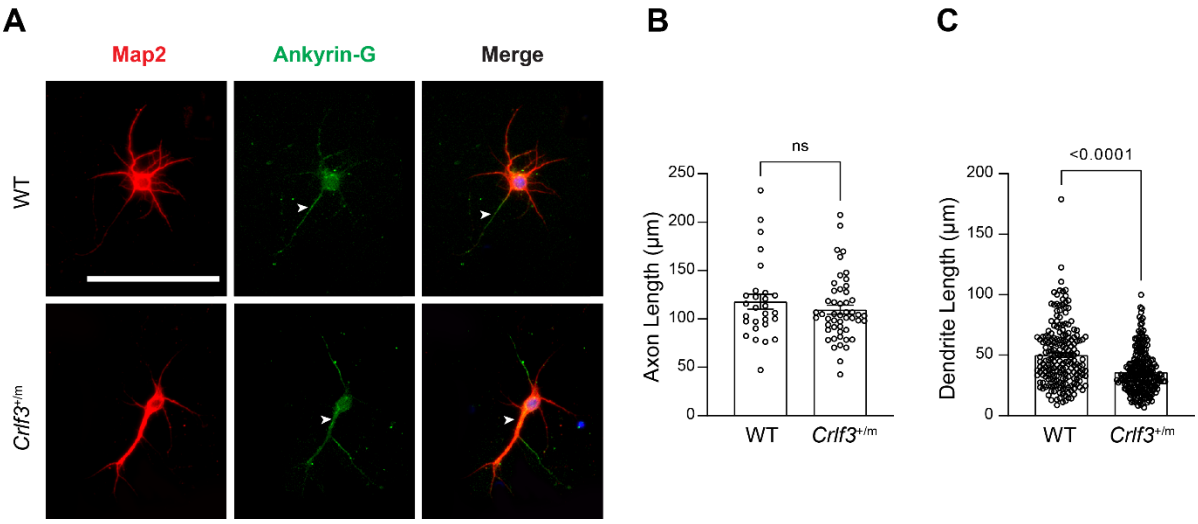

Supplemental Figure 4. *Crlf3*$^{+/m}$ hippocampal neurons have dendritic defects. (**A**) Representative images of 14 DIV mouse hippocampal neurons immunolabeled with Map2 (red) and ankyrin-G (green) prior to counterstaining with Hoechst-33258. The axons are denoted with white arrowheads. Scale bar: 100µm. (**B**) Axon lengths of *Crlf3*$^{+/m}$ hippocampal neurons are indistinguishable from wild type controls. (**C**) *Crlf3*$^{+/m}$ hippocampal neurons have reduced average dendrite lengths relative to wild type neurons. All data are shown as the mean ± SEM. Unpaired, two-tailed t-tests. P value is shown within the graph. ns, not significant.

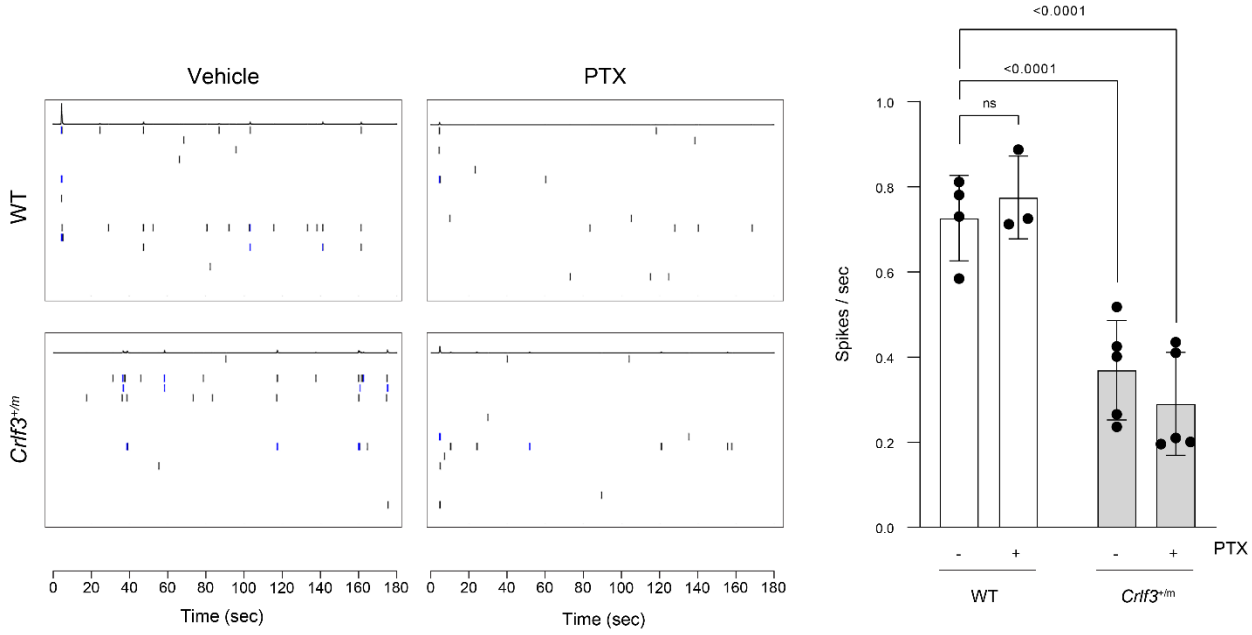

Supplemental Figure 5. *Crlf3*$^{+/m}$ hippocampal neurons have reduced firing rates that are unaffected by picrotoxin treatment. Representative traces and quantification from MEA recordings of *Crlf3*$^{+/m}$ and wild type hippocampal neurons in the presence or absence of picrotoxin (PTX). Each data point represents the average of 4 technical replicates from a single animal. Data are represented as the mean ±SEM. Two-way ANOVA with Dunnett's multiple comparisons test. ns, not significant.

Supplemental References

1 Chen, J., Lambo, M.E., Ge, X., Dearborn, J.T., Liu, Y., McCullough, K.B., Swift, R.G., Tabachnick, D.R., Tian, L., Noguchi, K. *et al.* (2021) A MYT1L syndrome mouse model recapitulates patient phenotypes and reveals altered brain development due to disrupted neuronal maturation. *Neuron*, **109**, 3775-3792 e3714.

2 Ehret, G. (2005) Infant rodent ultrasounds -- a gate to the understanding of sound communication. *Behav Genet*, **35**, 19-29.

3 Maloney, S.E., Chandler, K.C., Anastasaki, C., Rieger, M.A., Gutmann, D.H. and Dougherty, J.D. (2018) Characterization of early communicative behavior in mouse models of neurofibromatosis type 1. *Autism Res*, **11**, 44-58.

4 Holy, T.E. and Guo, Z. (2005) Ultrasonic songs of male mice. *PLoS Biol*, **3**, e386.

5 Rieger, M.A. and Dougherty, J.D. (2016) Analysis of within Subjects Variability in Mouse Ultrasonic Vocalization: Pups Exhibit Inconsistent, State-Like Patterns of Call Production. *Front Behav Neurosci*, **10**, 182.

6 Moy, S.S., Nadler, J.J., Perez, A., Barbaro, R.P., Johns, J.M., Magnuson, T.R., Piven, J. and Crawley, J.N. (2004) Sociability and preference for social novelty in five inbred strains: an approach to assess autistic-like behavior in mice. *Genes Brain Behav*, **3**, 287-302.

7 Nygaard, K.R., Maloney, S.E. and Dougherty, J.D. (2019) Erroneous inference based on a lack of preference within one group: Autism, mice, and the social approach task. *Autism Res*, **12**, 1171-1183.

8 Kopp, N., McCullough, K., Maloney, S.E. and Dougherty, J.D. (2019) Gtf2i and Gtf2ird1 mutation do not account for the full phenotypic effect of the Williams syndrome critical region in mouse models. *Hum Mol Genet*, **28**, 3443-3465.

9 Maloney, S.E., Yuede, C.M., Creeley, C.E., Williams, S.L., Huffman, J.N., Taylor, G.T., Noguchi, K.N. and Wozniak, D.F. (2019) Repeated neonatal isoflurane exposures in the mouse induce apoptotic degenerative changes in the brain and relatively mild long-term behavioral deficits. *Sci Rep*, **9**, 2779.

10 Palanisamy, A., Giri, T., Jiang, J., Bice, A., Quirk, J.D., Conyers, S.B., Maloney, S.E., Raghuraman, N., Bauer, A.Q., Garbow, J.R. *et al.* (2020) In utero exposure to transient ischemia-hypoxemia promotes long-term neurodevelopmental abnormalities in male rat offspring. *JCI Insight*, **5**.